

The Abnormal Threshold Anomaly in the ${}^6\text{Li} + {}^{208}\text{Pb}$ System

Z. J. Huang¹, C. J. Lin^{1,2,*}, L. Yang¹, H. M. Jia¹, F. Yang¹, N. R. Ma¹, P. W. Wen¹, T. P. Luo¹, C. Chang¹, H. R. Duan¹, S. X. Zhu¹, C. Yin¹, and J. H. Yang^{1,2}

¹China Institute of Atomic Energy, P. O. Box 275(10), Beijing 102413, China

²College of Physics and Technology & Guangxi Key Laboratory of Nuclear Physics and Technology, Guangxi Normal University, Guilin 541004, China

Abstract. Numerous studies have demonstrated that the phenomenological optical potential of tightly bound nuclear systems presents a threshold anomaly phenomenon in the near-Coulomb barrier energy region, where the relationship between the real and imaginary potentials can be well described by the dispersion relation. However, for some weakly bound nuclear systems, the phenomenological optical potential seems to manifest differently, and the dispersion relation struggles to describe the behavior between real and imaginary potentials. Recently, we measured the angular distributions of the transfer reaction ${}^{207}\text{Pb}({}^7\text{Li}, {}^6\text{Li}){}^{208}\text{Pb}$ in both near and deep barrier energy regions, as well as the elastic scattering angular distributions of the entrance channel ${}^7\text{Li} + {}^{207}\text{Pb}$. Optical potentials of the ${}^6\text{Li} + {}^{208}\text{Pb}$ system were extracted. The current results indicate that the optical potentials exhibit an abnormal threshold anomaly, and the dispersion relation is not applicable. Possible explanations are discussed, yet further investigations into the underlying physics are required.

1 Introduction

The optical model has been widely used in the field of nuclear physics and has achieved great success in the past seventy years. It is considered one of the most fundamental reaction models in nuclear physics. With development of the research, it has been found that the depths of the optical model potential (OMP) vary significantly near the Coulomb barrier with energy. In 1983, J. Lilley extracted optical potential parameters for the ${}^{16}\text{O} + {}^{208}\text{Pb}$ system through elastic scattering angular distributions [1]. They found that the optical potentials exhibit energy dependence near the Coulomb barrier: at the sensitive radius, the depths of the imaginary potentials decrease approximately linearly with decreasing energy, falling to zero in the sub-barrier energy region; while at the same time, the real potentials show an anomalous variation around the barrier. This phenomenon is called "threshold abnormality" (TA). Subsequently, the same phenomenon was observed in many other reaction systems [2–4]. Through long-term systematic studies, it has been gained: the imaginary potential approaches zero rapidly in the sub-barrier energy region, indicating that various reaction channels gradually close as the energy decreases and that there exists a threshold energy for reaction occurrence. The variation in the depth of the imaginary potential generates a dynamic polarization potential in the real potential, which ultimately also leads to changes in the depth of the real potential. The relationship between the changes in the depth of the imaginary and real potentials can be described by dispersion relations [5].

With the completion of the radioactive beam facility, researches on exotic nuclear structures and dynamics have become one of the hot topics in the field of nuclear physics. Compared to tightly bound nuclei, the optical potentials of both stable weakly bound nuclei and halo nuclei exhibit different patterns of variation near the potential barrier [6–9]: in these systems, as the incident energy decreases below the barrier, the depth of the imaginary potential does not approach zero quickly, but rather shows an increasing trend. We refer to this phenomenon as the anomalous threshold anomaly (ATA). An important question emerges: is the dispersion relation still applicable in these systems? This is currently still a highly controversial and hot issue. Our previous measurement of the optical potential for the ${}^6\text{He} + {}^{209}\text{Bi}$ system [10] in the complex potential region revealed that the dispersion relation is not applicable to this system. However, there is still a lack of experimental data for stable weakly bound nuclei such as ${}^6\text{Li}$ and ${}^9\text{Be}$ to allow for a deterministic conclusion to be drawn.

In general, optical potential parameters are extracted by fitting the angular distribution of elastic scattering. However, at energies close to or below the barrier, the angular distribution of elastic scattering becomes very flat, making it difficult to extract enough information from it. Therefore, a transfer reaction method [11] was proposed to study the OMPs of weakly bound nuclear systems. The principle of the transfer reaction method can be simply introduced as follows: For a transfer reaction $a + A \rightarrow b + B$ (assuming $a = b + x$ and $B = A + x$, the transferred particle x moves from a to A). The element of the transition matrix T can be derived from the Schrödinger equation when the optical potentials U_α and U_β for the entrance and

*e-mail: cjin@ciae.ac.cn

exit channels, as well as the bound state potential V_A (for $a = b + x$) and VB (for $B = A + x$) are known. So the differential cross section can be described as:

$$\left(\frac{d\sigma}{d\Omega}\right)_{\beta\alpha} = f(U_\alpha, U_\beta, V_A, V_B). \quad (1)$$

Therefore, if U_α , V_A and V_B are known exactly, the optical potential U_β for the entrance channel can be deduced by means of fitting the angular distribution of the transfer reaction. The sensitivity of this method has been investigated theoretically [12] and the results indicate that, except for some ambiguity in the real depth V at low energies the other parameters of the exit channels OMPs can be reliably extracted by fitting the transfer angle distribution. It is worth mentioning that as the energy further decreases, the sensitivity of this method will also decrease. Moreover, the reliability of this method also was confirmed experimentally in the previous works [13, 14].

In this work, we measured the angular distributions of elastic scattering for the ${}^7\text{Li}+{}^{207}\text{Pb}$ system and single-neutron transfer reaction ${}^{207}\text{Pb}({}^7\text{Li}, {}^6\text{Li}){}^{208}\text{Pb}$, with bombarding energies ranging from 21 MeV to 37 MeV. This experiment extracts the optical potential parameters of the ${}^6\text{Li}+{}^{208}\text{Pb}$ system based on the transfer reaction method developed by our group, to studies the energy dependence of the real and imaginary parts of the optical potential and obtains the reaction threshold energy in the deep barrier energy region.

2 Experimental setup

The experiment was carried out at the HI-13 tandem accelerator of the China Institute of Atomic Energy, Beijing. The accelerator provided a ${}^7\text{Li}$ beam with approximately 40 pnA intensity, bombarding on a ${}^{207}\text{Pb}$ target with a thickness of about $100 \mu\text{g}/\text{cm}^2$ on a $20 \mu\text{g}/\text{cm}^2$ carbon backing. Seven energy points of 21.98, 23.90, 25.81, 27.72, 31.54, 35.37, and 39.19 MeV in the laboratory system were measured.

Two Si-detector telescopes were fixed on a plate that can rotate around the target, to achieve measurements of large angles ranging from 30° to 170° . Each group of telescopes consists of two layers of Si detectors. The first layer is a $40 \mu\text{m}$ double-side strip detector (16×16 pixels) with an active area of $50 \times 50 \text{ mm}^2$ as the ΔE detector. The second layer is a $1000 \mu\text{m}$ quadrant silicon detector (2×2 pixels) with the same active area for measuring the remaining energy E_R . Besides, two PIN detectors were placed at $\pm 15^\circ$ as monitors to measure pure Rutherford scattering, which is used for relative normalization of the differential cross section.

3 Data Analysis

3.1 Elastic scattering of ${}^7\text{Li} + {}^{207}\text{Pb}$

The elastic scattering angular distribution (normalized to the Rutherford cross section) of ${}^7\text{Li}+{}^{207}\text{Pb}$ at all energies obtained in the experiment is shown in Fig.1. To

obtain a reliable optical potential for the ${}^7\text{Li}+{}^{207}\text{Pb}$ system, a simultaneous fit of the six parameters $\{X_i\} = \{V, r_V, a_V, W, r_W, a_W\}$ of the optical potential was performed by the code FRESCO [15]. In the fitting procedure, a grid search on all the six potential parameters was carried out to obtain the best fit to the angular distributions at different bombarding energies. For each angular distribution of N data points, the goodness of fit quantity χ^2 was calculated as Eq.(1).

$$\chi^2/\text{pt} = \frac{1}{N} \sum_{i=1}^N \left(\frac{\sigma_i^{\text{exp}} - \sigma_i^{\text{the}}}{\delta\sigma_i^{\text{exp}}} \right)^2. \quad (2)$$

where σ_i^{the} , σ_i^{exp} and $\delta\sigma_i^{\text{exp}}$ are the calculated cross section, the experimental cross section, and its associated error at each angle θ_i , respectively. The obtained optimal optical potential parameters and χ^2/pt values are listed in Table 1. The fitting results are shown in Fig.1 by the red solid curves, it can be seen that they fit the experimental angular distributions quite well.

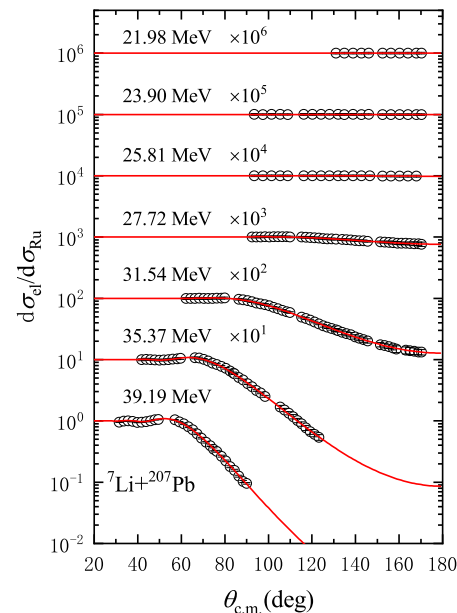


Figure 1. Elastic scattering angular distributions of the ${}^7\text{Li}+{}^{207}\text{Pb}$ system at different energies. The circular dots represent experimental data, and the red solid line is the fitting result by the optical model.

3.2 OMPs of ${}^6\text{Li} + {}^{208}\text{Pb}$ system

The angular distribution of the ${}^{207}\text{Pb}({}^7\text{Li}, {}^6\text{Li}){}^{208}\text{Pb}$ transfer reaction obtained from the experiment is shown in Fig.2. Only the statistical errors are considered for the experimental data. At lower energy points below 25.81 MeV, the experiment observed only the transfer reaction final states where neutrons were transferred from ${}^7\text{Li}$ to the ground state of ${}^{208}\text{Pb}$. As the reaction energy increased, at incident energies of 27.72, 31.54, and 35.37 MeV, in addition to the ground state-to-ground state transfer reaction process, the reaction final states where neutrons were

Table 1. The OMP parameters extracted from the elastic scattering data of the ${}^7\text{Li}+{}^{207}\text{Pb}$ system

E_{lab} MeV	V MeV	r_V fm	a_V fm	W MeV	r_W fm	a_W fm	χ^2/pt
39.19	14.19	1.32	0.56	15.98	1.28	0.67	4.53
35.37	15.35	1.35	0.54	15.88	1.32	0.60	4.57
31.54	23.01	1.30	0.59	12.03	1.34	0.66	3.08
27.72	27.14	1.25	0.71	12.34	1.34	0.52	3.37
25.81	14.29	1.37	0.51	3.06	1.27	0.58	2.61
23.90	12.61	1.27	0.64	4.07	1.21	0.59	3.55
21.98	4.72	1.22	0.62	3.74	1.20	0.60	4.45

transferred to the 3.197 and 3.475 MeV excited states of ${}^{208}\text{Pb}$ were also observed. The results are shown as triangles and rhombuses in Fig.2.

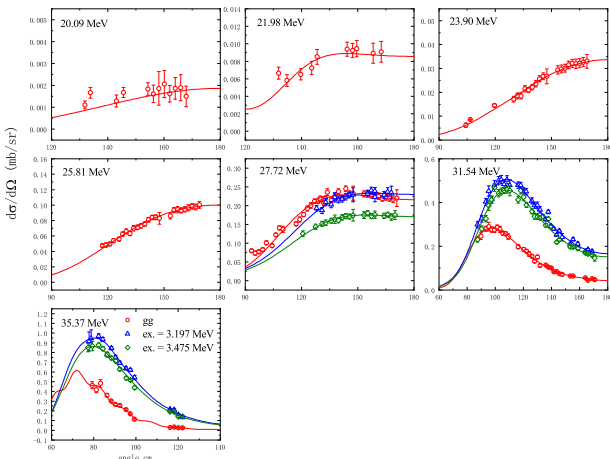


Figure 2. Angular distributions of the ${}^{207}\text{Pb}({}^7\text{Li},{}^6\text{Li}){}^{208}\text{Pb}$ transfer reactions. The red open circles, blue triangles, and green diamonds represent the experimental results of neutron transfer to the ground state (gg), the excited states at 3.197 MeV and 3.475 MeV of ${}^{208}\text{Pb}$, respectively. The solid curves are the results of fitting by the CRC method.

In order to extract the optical potential parameters of the exit channel ${}^6\text{Li}+{}^{208}\text{Pb}$, the coupled reaction channels (CRC) calculation was employed to fit the ${}^{207}\text{Pb}({}^7\text{Li},{}^6\text{Li}){}^{208}\text{Pb}$ transfer reaction. The coupled-channels method describes the effects of non-elastic and other reaction channels on the elastic channel by solving a set of coupled channel equations, and further considering the coupling effects between different reaction channels. The optical potentials for the entrance channel were fitted using the optical model based on the elastic scattering data of ${}^7\text{Li}+{}^{207}\text{Pb}$; while for the exit channel, the radii and diffuseness parameters were fixed at $r_V = 1.15$ fm, $r_W = 1.30$ fm and $a_V = 0.66$ fm, $a_W = 0.60$ fm, respectively. In order to investigate the energy dependence of the optical potential of the ${}^6\text{Li}+{}^{208}\text{Pb}$ system, the diffuseness parameters a_V and a_W were changed separately with a step size of 0.02 fm to extract the sensitivity radius R_s , while the depth values were fitted again [17]. For both the real and imaginary parts of the potential, the average

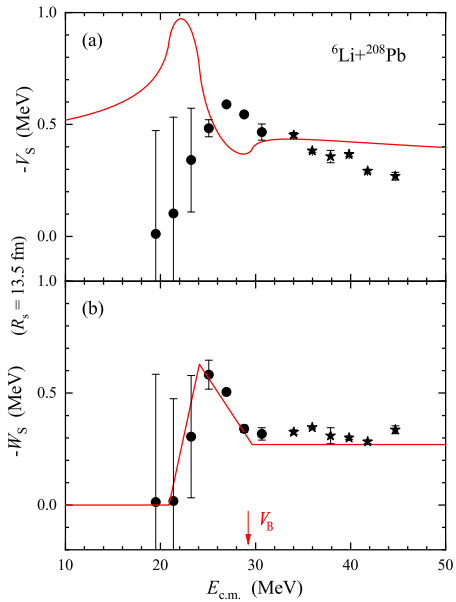


Figure 3. Energy dependence of the real (a) and imaginary (b) potentials at the sensitivity radius of 13.5 fm for the ${}^6\text{Li}+{}^{208}\text{Pb}$ system. The present results are shown by the circles, and asterisks represent the results taken from Ref. [16]. The solid curve in (b) shows the linear segment fitting for the imaginary potential. The prediction of the dispersion relation according to the variation of the imaginary potential is present in (a) by the solid curve.

sensitivity radius was found to be $R_s = 13.5$ fm. All calculations were performed using the FRESCO code [15]. The real and imaginary parts of the optical potential at the sensitivity radius of 13.5 fm for the ${}^6\text{Li}+{}^{208}\text{Pb}$ system is shown in Fig.3, where the data at high energies from Ref.[16] are shown by asterisks. Moreover, The errors of potential depths were derived by χ^2 analysis with a confidence level of 68.3%. One can find that the errors become large for the sub-barrier-energy range. This indicates that the interactions below the Coulomb barrier may not be as sensitive to the depth of the OMP as those above the barrier. For the depths of the imaginary potential, there is a gradually rising trend as the incident energy decreases. When the incident energy is below the Coulomb barrier (~ 29 MeV), the depth of the imaginary potential begins to decrease gradually and approaches zero quickly, indicating that there exists a threshold for reactions to occur. For the real part depths, it exhibits a bell-shaped curve near the barrier. These results are very similar to those for the ${}^6\text{He}+{}^{209}\text{Bi}$ system, representing a typical abnormal threshold anomaly phenomenon.

Additionally, the applicability of the dispersion relation in this system was also investigated. As shown by the solid line in Fig.3(a), we use a simple linear model to describe the imaginary potential, the real part is obtained through the dispersion relation [18], as shown by the solid curve in Fig.3(b). Comparing with the experimental results, it is clearly shown that the dispersion relation for ${}^6\text{Li}+{}^{208}\text{Pb}$ does not hold, which is also presented in other weakly bound systems [19, 20].

The dispersion relation is based on the causality principle as manifested in the Kramers-Kronig relation, which is obtained from Cauchys residue theorem. To satisfy the derivation conditions, it is required that the complex plane should contain a series of isolated singularities corresponding to the discrete states of interacting nuclear systems. In the case of exotic nuclear systems, the existence of a continuum state due to the breakup process clearly does not satisfy the requirements of the residue theorem. Therefore, the direct application of the dispersion relation to exotic nuclear systems is not mathematically rigorous. It is necessary to found a new relationship that describes the anomalous behavior between the real and imaginary potentials of weakly bound nuclear systems with continuous states.

4 Summary and Conclusions

In conclusion, the angular distributions of the transfer reaction $^{207}\text{Pb}(^7\text{Li}, ^6\text{Li})^{208}\text{Pb}$ were measured at near-barrier and sub-barrier energies, as well as the elastic scattering angle distributions of the entrance channel $^7\text{Li}+^{207}\text{Pb}$. The optical potential parameters of the weakly bound system $^6\text{Li}+^{208}\text{Pb}$ were extracted by fitting the experimental data within the CRC framework. Preliminary results indicate that the real and imaginary parts of the optical potential as functions of bombardment energy exhibited a clear abnormal threshold anomaly. Moreover, the classical dispersion relation cannot be used to describe the relationship between the real and imaginary parts. We have discussed possible reasons for this particular behavior, but further research is needed to uncover the underlying physics.

5 Acknowledgments

This work was supported by the National Key Basic Research Program of China (Grant Nos. 2022YFA1602302 and 2023YFA1606402) and the National Natural Science Foundation of China (Grants Nos. 12235020, 12275360, U2167204, and 12175313).

References

- [1] J. S. Lilley, B. R. Fulton, M. A. Nagarajan, I. J. Thompson, and D. W. Banes, Phys. Lett. **151B**, 181 (1985).
- [2] B. R. Fulton, D. W. Banes, J. S. Lilley et al., Phys. Lett. B **162**, 55 (1985).
- [3] G. R. Satchler, Phys. Rep. **199**, 147 (1991).
- [4] P. Singh, S. Kailas, A. Chatterjee et al., Nucl. Phys. A **555**, 606 (1993).
- [5] M. A. Nagarajan, C. C. Mahaux, and G. R. Satchler, Phys. Rev. Lett. **54**, 1136 (1985).
- [6] N. Keeley, R. Raabe, N. Alamanos, and J. Sida, Prog. Part. Nucl. Phys. **59**, 579 (2007).
- [7] N. Keeley, S. J. Bennett, N. M. Clarke et al., Nucl. Phys. A **571**, 326 (1994).
- [8] Hussein M. S., Gomes P. R. S., Lubian J., et al., Phys. Rev. C **73**(4), 044610 (2006).
- [9] Niello J. O. F., Figueira J. M., Abriola D., et al., Nucl. Phys. A **787**(1-4), 484 (2007).
- [10] L. Yang, C.J. Lin, H.M. Jia et al., Phys. Rev. Lett. **119**, 042503 (2017).
- [11] C. J. Lin, F. Yang, P. Zhou, H. Q. Zhang, Z. H. Liu, M. Ruan, X. K. Wu, and C. L. Zhang, AIP Conf. Proc. **853**, 81 (2006).
- [12] Wu Zhen-Dong, Yang Lei, Lin Cheng-Jian et al., Chin. Phys. Lett. **31**, 092401 (2014)
- [13] L. Yang, C.J. Lin, H.M. Jia et al., Phys. Rev. C **89**, 044615 (2014).
- [14] L. Yang, C. J. Lin, H. M. Jia et al., Phys. Rev. C **95**, 034616 (2017)
- [15] I. J. Thompson, Computer Physics Reports **7**, 167 (1988).
- [16] Zhang Chun-Lei et al., Chin. Phys. Lett. **23**, 1146 (2006).
- [17] C. J. Lin, J. C. Xu, H. Q. Zhang, Z. H. Liu, F. Yang, and L. X. Lu, Phys. Rev. C **63**, 064606 (2001).
- [18] C. Mahaux, H. Ngô, and G. R. Satchler, Nucl. Phys. A **449**, 354 (1986).
- [19] R. Lipperheide and A. K. Schmidt, Nucl. Phys. A **112**, 65 (1968).
- [20] A. Pakou, N. Alamanos, G. Doukelis et al., Phys. Rev. C **69**, 054602 (2004).